Femtosecond Photolysis of ClO_2 in Aqueous Solution

J. Thøgersen, P. U. Jepsen, C. L. Thomsen, J. Aa. Poulsen, J. R. Byberg, and S. R. Keiding*

Department of Chemistry, University of Aarhus, Langelandsgade 140, DK-8000 Aarhus C, Denmark

Received: October 18, 1996[⊗]

The photolysis of aqueous ClO_2 has been studied with a new femtosecond transient absorption spectrometer, allowing absorbance changes as small as $\Delta A \approx 1 \times 10^{-4}$ to be recorded with a time resolution of 150 fs. ClO_2 was photolyzed at 390 nm and the ultrafast formation and decay of photoproducts were monitored at 260, 390, and 780 nm. As expected from earlier studies, Cl atoms are formed with a quantum yield of $\Phi(Cl) = 0.1$. However, the rate of formation is nearly 2 orders of magnitude higher than that reported. Moreover, Cl is the *only* photoproduct that survives 25 ps after the photolysis pulse. The main photolytic products, ClO + O, formed with a quantum yield of 0.9, disappear through fast geminate recombination, producing vibrational excited ClO_2 in the electronic ground state. The vibrational relaxation of this species occurs with a time constant of 10 ps. The vanishing yield of cage escape for ClO + O, which contrasts with the reported result of the photolysis at 355 nm, indicates that the amount of excess energy imparted to these products at 390 nm is insufficient to enable them to separate. The decay of a photoinduced dichroism observed at 390 nm is interpreted as an orientational relaxation of ground-state ClO_2 , the time constant (0.6 ps) agreeing with that calculated from the hydrodynamical slip model.

Introduction

The involvement of chlorine dioxide (ClO_2) in the photochemical processes leading to ozone depletion in the upper atmosphere has been much debated. When ClO_2 is photolyzed in the gas phase with near-ultraviolet light, the dominant products are ClO + O,which do not cause a net removal of ozone. It has been suggested,[1] however, that photolytic formation of Cl + O_2 via isomerization to ClOO could contribute significantly to the catalytic destruction of ozone. A moderate yield of chlorine atoms from the photolysis of ClO_2 in the gas phase has been confirmed experimentally,[2−5] whereas the intermediate formation of ClOO is still controversial.

The current understanding of the photoreactivity of ClO_2 in the gas phase as well as in liquid solution has recently been reviewed by Vaida and Simon.[6] The description of the photolysis of ClO_2 in solution is based on several detailed flash photolysis experiments with picosecond time resolution by Simon and co-workers.[7−10]

The photolysis in the near-UV region is initiated by exciting ClO_2 from the $^2B_1$ ground state to the $^2A_2$ state, which couples to the nearby $^2A_1$ and $^2B_2$ states through spin−orbit and vibronic interactions. In the liquid phase these processes are thought to be faster than the reactive changes, so the photochemistry of ClO_2 originates from the $^2B_2$ state. Three competitive reactions take place:

$$ClO_2(^2B_2) \rightarrow ClO(^2\Pi) + O(^3P) \quad (90\%) \qquad (1)$$

$$ClO_2(^2B_2) \rightarrow O_2(^1\Delta_g) + Cl(^2P) \quad (0.5\%) \qquad (2)$$

$$ClO_2(^2B_2) \rightarrow ClOO \rightarrow O_2(^3\Sigma^-_g) + Cl(^2P) \quad (9.5\%) \qquad (3)$$

The reported distribution among the three reaction channels in aqueous solution is indicated in parentheses. Since no fast regeneration of ClO_2 was considered, these figures represent the quantum yields. The ratio of the yields of reactions 1 and 3 was derived from a kinetic model fitted to the time evolution of the observed transient absorptions,[8] whereas the yield of reaction 2 was measured directly.[10] These results indicate that 5% of the chlorine atoms stem from direct elimination along a reaction coordinate of C_{2v} symmetry, while the remaining chlorine atoms arise from the photoisomerization of ClO_2 to ClOO followed by a slow thermal decomposition into Cl + O_2. The lifetime reported for ClOO in water is 150 ps. The products of the dominant reaction 1 recombine to ClO_2 on a nanosecond time scale.[8]

The direct formation of ClOO in the electronic ground state from the excited $^2B_2$ state of ClO_2 implied by reaction 3 is intriguing because the correlation diagram based on orbital symmetry suggests that ClOO should be formed in an excited state,[9] and the excited states of ClOO are thought to be dissociative.[11] Therefore, recombination of Cl and O_2, which is known to yield ClOO in the gas phase,[12,13] would seem to be a more likely source of ground-state ClOO. The occurrence of direct photoisomerization of ClO_2 to ClOO has yet to be unambiguously established.

The present investigation of the photolysis of aqueous ClO_2 was originally undertaken to study the mechanism of formation of ClOO. Transient absorption data were obtained on a common scale at 260, 390, and 780 nm, allowing us to monitor with femtosecond time resolution the bleaching of ClO_2 and the transient concentrations of Cl, ClO, and ClOO, as well as the relaxation of products formed in vibrationally excited states. The data obtained at 260 nm are particularly well suited for studying the formation and decay of ClOO because this species absorbs very strongly at 260 nm.[12−14]

In a very recent paper, Chang and Simon described similar femtosecond photolysis experiments on aqueous ClO_2.[15] They used probe wavelengths in the range 350−700 nm to monitor the transient absorption of the photoproducts. The transients observed in the visible region were assigned to vibrationally excited ClOO formed within the duration of the pump pulse. Although our results at 390 and 780 nm are fully consistent with the data reported by Chang and Simon, our additional data at 260 nm are incompatible with the proposed formation of ClOO and, hence, lead to a somewhat different description of

* To whom correspondence should be addressed (e-mail: keiding@kemi.aau.dk).

⊗ Abstract published in *Advance ACS Abstracts,* April 1, 1997.

S1089-5639(96)03230-6 CCC: $14.00

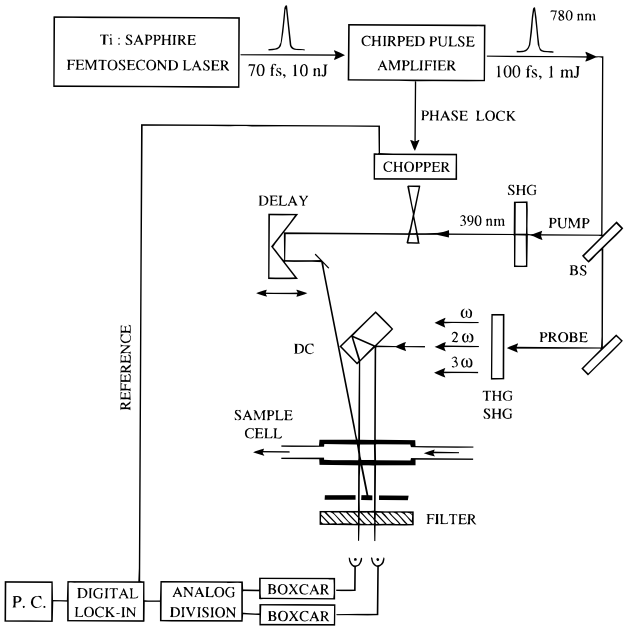

Figure 1. Experimental setup.

the primary photolysis of aqueous ClO_2, involving instead vibrationally excited ClO_2 formed by fast geminate recombination of O + ClO. The analysis of the present results suggests that Cl and O_2 are the only products escaping the cage after excitation at 390 nm, whereas ClO is the dominant product detected after excitation at 355 nm.[8] This wavelength dependence of the effective quantum yield of ClO is discussed in terms of potential curves of the pertinent excited states of ClO_2.[16] The observed photodynamics of aqueous ClO_2 is compared to that found recently in a similar femtosecond study of the isoelectronic and isostructural species O_3^-.[17]

Experimental Section

Aqueous solutions of ClO_2 were initially prepared by the method described by Bray.[18] Oxalic acid (Riedel-deHaën, chemical pure) and potassium chlorate (Merck, analytical grade) were mixed and heated to 60 °C, and a few drops of water were added to initiate the reaction. The resulting gaseous mixture of ClO_2 and CO_2 was bubbled through three times destilled water. The desired concentration of ClO_2 was reached within 1 h. To make sure that residual impurities did not distort the results obtained, we repeated the experiments with solutions of ClO_2 prepared by an alternative method.[19] $NaClO_2$ and $K_2S_2O_8$ (Fluka, analytical grade) were mixed and a few drops of water were added. The gaseous reaction products were diluted with pure nitrogen, led through 0.1 M aqueous $NaClO_2$ to remove residual Cl_2, and subsequently bubbled through three times destilled water. The resulting highly pure ClO_2 solution was stable for several weeks when kept in the dark. Some caution with this synthesis is required, since small explosions can occur. The experimental results obtained were independent of the method of synthesis.

The experimental setup is shown schematically in Figure 1. A regeneratively amplified Ti:sapphire laser from CLARK-MXR with a repetition rate of 1 kHz was employed in this work. The output from the amplifier is 100 fs pulses with a wavelength centered at 780 nm and a pulse energy of ∼0.7 mJ. Part of the fundamental beam was frequency doubled in a 0.2 mm BBO crystal to give the 390 nm pulse used for the photolysis of ClO_2, hereafter denoted as the pump pulse. Part of the 390 nm pulse was combined with the remainder of the fundamental beam in a 0.1 mm BBO crystal to give a 260 nm pulse by sum-frequency mixing. The energy of the pump pulse at 390 nm was 30, 78, and 42 μJ when probing at 260, 390, and 780 nm, respectively, and the radius of the spot of the weakly focused pump beam was measured at the sample to be 0.4 mm by means of a scanning knife's edge. Before passing through the sample, the probe beam was divided into a signal and a reference beam by a 10 mm quartz window inserted at 45°. The pump beam crossing the signal beam at an angle of ∼5° was modulated at 0.5 kHz, phase-locked to the 1 kHz repetition rate of the regenerative amplifier. The spot size of the signal beam was made smaller than that of the pump beam to ensure an optimum overlap of the two beams at the sample. After passing the sample, the pump and the probe beams were spatially separated with iris diaphrams, and the signal and the reference beams were spectrally filtered by quartz dispersion prisms before they were detected by two matched photodiodes and boxcar integrators. The ratio of the signals from the two boxcar integrators was sent to a digital lock-in amplifier referenced to the pump beam modulation. With this detection scheme, absorbance changes smaller than 1×10^{-4} could be observed. In the measurements of rotational anisotropy of ClO_2, the relative polarization of the pump and probe beams was controlled with a Soleil-Babinet compensator inserted in the pump beam. Thus, the polarization of the pump beam could be changed without disturbing the alignment.

The sample solution was pumped through a 2 mm quartz cuvette. The concentration of ClO_2 was approximately 7 mM, corresponding to an optical density of 1 in the cuvette at 390 nm, and the flow rate was adjusted to ensure a fresh sample of ClO_2 for each laser pulse. A typical scan was recorded in 15 min. No degradation of the ClO_2 solution was observed on this time scale.

Photolysis at 390 nm of a sample of pure water gave a sharp transient absorption signal at all probe wavelengths. This transient can be assigned to two-beam coupling.[20] Assuming the optical response of pure water to be instantaneous, we used these signals to characterize the pump and probe pulses. For the 390 nm probe, the water transient is well represented by the cross correlation of two Gaussian pulses with a fwhm equal to 150 fs. This is in agreement with the temporal broadening of 100 fs pulses caused by dispersion in the optical components and the sample cell. For the 260 and 780 nm probes, the time resolution was reduced to approximately 0.4 ps by the large group velocity dispersion in the experimental setup between the pump and the probe at these wavelengths.

A series of experiments, in which the power of the pump pulse was changed by more than 1 order of magnitude, showed that the photoinduced changes of absorbance were proportional to the pump power. This indicates that hole-burning in the absorption band of ground-state ClO_2 and two-photon absorption are insignificant. The measurements also showed that the photodynamics was independent of the pump power. The photoinduced changes of the absorbance were brought on a common scale by normalizing the observed transients to a fixed power of the pump pulse. The pump power was measured with a Coherent Lasermate 10 power meter, which has an accuracy of ±10%. From numerous measurements we found the alignment reproducibility to be better than ±20%. We therefore estimate the relative values of the normalized absorbances at 260, 390, and 780 nm to be accurate to within ±25% .

Results

Description of Transient Data. The changes $\Delta A(\lambda,t)$ in the absorbance of aqueous ClO_2, produced by the 390 nm pump

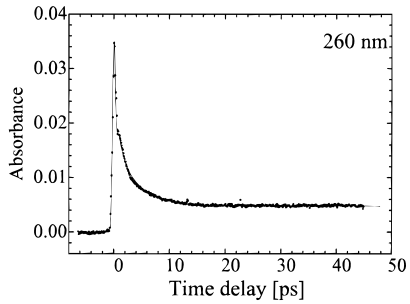

Figure 2. Transient absorption at 260 nm produced in aqueous ClO_2 by the 390 nm pump pulse of width 150 fs and recorded as function of the delay t after the pulse with perpendicular polarizations of pump and probe beams. Solid circles indicate the measured absorption, while the continous curve represents the absorption calculated from the proposed mechanism (eq 9, Table 2), with a sharp peak added at $t = 0$ to account for the two-beam coupling of pump and probe.

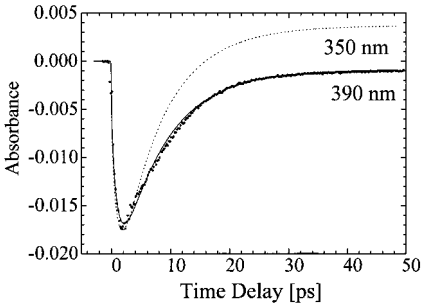

Figure 3. Transient absorption data at 390 nm (see caption to Figure 2). The dashed curve represents the transient absorption at 350 nm as predicted from eq 9 and Table 2.

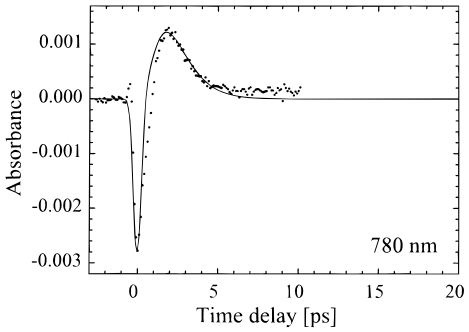

Figure 4. Transient absorption data at 780 nm (see caption to Figure 2).

pulse and measured at the wavelengths $\lambda = 260$, 390, and 780 nm with the polarizations of pump and probe beams perpendicular to each other, are shown in Figures 2−4 as functions of the time delay t after the pump pulse. Each curve displays an initial sharp peak resembling closely that obtained at the same wavelength when pure water is substituted for the ClO_2 solution without changing the alignment of the setup. Hence, we ascribe this peak to the two-beam coupling associated with the solvent and take the temporal position of the peak to mark the point of zero delay ($t = 0$). Apart from this initial signal from the solvent, ΔA(260 nm) (Figure 2) rises to a maximum at 0.5 ps delay and exhibits two distinct decays with time constants near 0.5 and 5 ps, respectively, reaching an almost constant level within 15 ps.

At 390 nm a strong initial bleaching is observed (Figure 3), which attains a maximum 2 ps after the photolysis pulse, and then decays with a time constant of 10 ps, leveling off at a near-zero value for $t > 50$ ps. The level at long delays is very sensitive to the wavelength of the probe pulse: when the laser is tuned to a wavelength slightly shorter than 390 nm, the weak

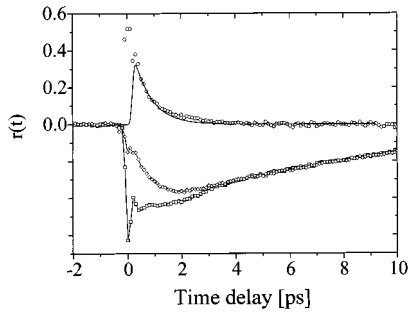

Figure 5. Absorptions recorded with perpendicular ($\Delta A_\perp$) and parallel ($\Delta A_\parallel$) polarizations of pump and probe beams shown as diamonds and squares, respectively. The anisotropy $r(t)$ defined by eq 4 is shown as circles. The continuous curve represents $r(t)$ in terms of the function $0.4 \exp(-(t - 0.3 \text{ ps})/0.6 \text{ ps})$ convolved with the pulse shape.

bleaching is replaced by a weak induced absorption. The strong initial bleaching indicates that the primary photoproducts, including the pertinent excited states of ClO_2, all absorb much less at 390 nm than does ClO_2 in the $^2B_1$ ground state. The nearly complete, fast recovery of the absorption at 390 nm, also observed by Chang and Simon,[15] contrasts with the earlier observations of Dunn and Simon,[8] who found a strong bleach at 385 and at 420 nm that persisted for several nanoseconds. This apparent discrepancy may be attributed to the different wavelengths of the photolysis pulses used in the femtosecond and picosecond experiments (390 and 355 nm, respectively) as discussed below.

At 780 nm the signal from the solvent is a negative peak (Figure 4), while ΔA(780 nm) associated with the photolysis of ClO_2 exhibits a small increase in absorbance, attaining a maximum at 2.1 ps, and subsequently decays with a time constant of 2 ps. A very small photoinduced absorbance persists at longer delays.

Polarization Measurements. The transient absorptions recorded at 260 and 780 nm with parallel polarization of the pump and probe beams were indistinguishable from the those shown in Figures 2 and 4, indicating the absence of polarization effects at these wavelengths. However, at 390 nm a marked photoinduced dichroism is observed at short delays. Figure 5 displays the transient absorptions $\Delta A_\perp$ and $\Delta A_\parallel$ obtained with perpendicular and parallel polarizations of the 390 nm pump pulse with respect to the 390 nm probe pulse, respectively. Also shown is the anisotropy $r(t)$ defined as

$$r(t) = \frac{\Delta A_\parallel(t) - \Delta A_\perp(t)}{\Delta A_\parallel(t) + 2\Delta A_\perp(t)} \qquad (4)$$

The anisotropy decays exponentially with a time constant of 0.6 ps.

Discussion

Comparison with Reported Quantum Yields. In accordance with previous work[8] the present results are interpreted in terms of the photolytic products Cl, ClO, and ClOO, which we assume have become fully thermalized at 25 ps after the pump pulse so that the extinction coefficients ϵ_i of the equilibrated species apply. The pertinent values are listed in Table 1. We note that the absorption spectrum of ClOO has not been measured in aqueous solution. An accurate UV spectrum in the gas phase has been obtained,[13] and a spectrum extending into the visible region has been measured in solid neon.[14] These spectra agree within the limit of error,[14] thus indicating the absence of large effects of the medium. Accordingly, we adopt the gas-phase value for the extinction coefficient

TABLE 1: Extinction Coefficients of ClO_2, Cl, ClO, and ClOO in Aqueous Solution

	ϵ [L cm^{-1} mol^{-1}]			
	260 nm	350 nm	390 nm	780 nm
ClO_2[a]	40	900	780	0
Cl[b]	2100	2500	430	0
ClO[c]	750	0	0	0
ClOO[d]	13000	≤300	≤200	0

[a] Estimated from the spectrum reported in ref 8, which was calibrated with extinction coefficients from ref 21. [b] Estimated from the spectrum reported in ref 22. [c] Estimated from the spectrum reported in ref 22, which was calibrated with the extinction coefficient from ref 23. [d] ϵ(260 nm) is the gas-phase value (ref 13), while ϵ(350 nm) and ϵ(390 nm) are estimated from the spectrum in solid neon (ref 14).

at 260 nm and estimate an upper limit for the extinction coefficient at 390 nm from the solid-state spectrum.

Since the absorbance changes ΔA(260 nm) and ΔA(390 nm) are measured on a common scale, both represent the chemical composition of the same photolyzed solution at any time. Taking the maximum bleaching at 390 nm (ΔA(390 nm) = −0.02; see Figure 3) to indicate the initial, photoinduced deficit of ground-state ClO_2 and, hence, the initial concentration of photoexcited ClO_2, we obtain $\Delta[ClO_2] = -0.02/(\epsilon_{ClO_2}(390\text{ nm}) \times d) = -1.3 \times 10^{-4}$ M, where d is the thickness of the sample in cm and ϵ_{ClO_2} is the extinction coefficient of ClO_2 (Table 1). In the absence of significant hole-burning, the absolute value of $\Delta[ClO_2]$ is a lower limit because we have assumed that none of the photoproducts or excited states of ClO_2 present at $t = 2$ ps absorb at 390 nm. Using the quantum yields reported by Dunn and Simon[8] for reactions 1−3, the reported lifetime of ClOO (150 ps), and the extinction coefficients of Table 1, we may then calculate ΔA(260 nm) at 25 ps, when all species have attained equilibrium. We find ΔA(260 nm) = 0.03, which is *6* times the observed value (ΔA(260 nm) = 0.005; see Figure 2). This discrepancy immediately suggests that the reported quantum yields do not apply to the present experiments.

Interpretation of the Asymptotic Behavior at Long Delays of the Transients at 390 and 260 nm. Among the species considered here, only ClO_2 and Cl have significant absorptions at 390 nm when in equilibrium with the solvent (Table 1). Hence, ΔA (390 nm) may be expressed in terms of the concentration of Cl atoms and the deficit of ClO_2. Since the values of ϵ_{ClO_2} and ϵ_{Cl} are similar at 390 nm, the near vanishing of ΔA at $t > 50$ ps suggests that the net photolysis of ClO_2 amounts to a conversion to $Cl + O_2$:

$$OClO \xrightarrow{h\nu} Cl + O_2 \qquad (5)$$

Specifically, very little ClO may survive because the corresponding deficit of ClO_2 would imply a substantial negative ΔA at long delays. Thus, the decay of the strong initial bleaching may be taken to represent a fast regeneration of ground-state ClO_2 via recombination of ClO and O, and the formation of Cl. Owing to the similarity of ϵ_{ClO_2} and ϵ_{Cl}, the extent of conversion in reaction 5 cannot be determined accurately at 390 nm. However, the transient $\Delta A(t)$ measured at 350 nm by Chang and Simon[15] contains the required information. Ignoring at this stage that ClOO has a moderate absorption at 350 nm ($\epsilon_{ClOO} \le 400$ M^{-1} cm^{-1}) and hence might contribute to the observed ΔA, we assume that ΔA may be expressed simply as

$$\Delta A = \{\epsilon_{Cl}[Cl] + \epsilon_{ClO_2}\Delta[ClO_2]\}d \qquad (6)$$

At long delays we may take $[Cl] \approx |\Delta[ClO_2]|$ as discussed above. The ratio $\Delta A(350\text{ nm})_{t=0}/\Delta A(350\text{ nm})_{t=60ps}$ estimated from Figure 1 of ref 15 is −4. Using eq 6, we thus obtain

$$-4 = \frac{\epsilon_{Cl}[Cl]_{t=0} + \epsilon_{ClO_2}\Delta[ClO_2]_{t=0}}{[Cl]_{t=60ps}}(\epsilon_{Cl} - \epsilon_{ClO_2})$$

To calculate from this expression the quantum yield for formation of Cl atoms, defined as $\Phi(Cl) \equiv [Cl]_{t=60ps}/\Delta[ClO_2]_{t=0}$, a value must be assumed for the unknown initial concentration $[Cl]_{t=0}$. With the extreme choices $[Cl]_{t=0} = 0$ and $[Cl]_{t=0} = [Cl]_{t=60ps}$, we obtain $\Phi(Cl) = 0.10$ and $\Phi(Cl) = 0.14$, respectively.

These quantum yields may be checked against our data at 260 nm. The calculated contributions of Cl to ΔA(260 nm) are 0.0051 and 0.0065, respectively, which are both consistent with the value of ΔA(260 nm) = 0.005 measured at 40 ps. We thus find that a quantum yield $\Phi(Cl) = 0.1$ agrees with the existing femtosecond observations. We note that this result is also in accord with the reported yield of Cl atoms arising from the slow thermal dissociation of ClOO found in the picosecond photolysis at 355 nm.[8] However, because the calculated absorption of Cl already tends to exceed the observed value of ΔA(260) at 40 ps delay, no ClOO seems to be present at that time, in agreement with the near-vanishing of ΔA(390 nm), and there is no room for a contribution from ClO at long delays. Hence, we conclude that 40−60 ps after the photolysis pulse of $\lambda = 390$ nm, about 10% of the initially excited ClO_2 have dissociated into $Cl + O_2$ while the remaining 90% have returned to the ground state of ClO_2.

The surprising result that no ClO is detected at long delays ($t > 25$ ps) in the photolysis of aqueous ClO_2 at 390 nm, whereas ClO is a major product of the photolysis at 355 nm and, moreover, persists after several nanoseconds,[8] may be interpreted within the framework of the potential curves for the excited states of ClO_2 obtained from the high-level ab initio calculations by Peterson and Werner.[16] The curves reproduced in Figure 6 represent the effect of an asymmetric distortion. As indicated in the figure, photoexcitation of $ClO_2(^2B_1)$ at 355 nm generates $ClO_2(^2A_2)$ with an energy that exceeds the height of the barrier in the ClO + O channel. Therefore, dissociation may occur directly from the $^2A_2$ state, yielding products with an excess energy of about 1.2 eV, which will enable them to acquire sufficient kinetic energy to escape the solvent cage. Recombination will in this case be a slow, diffusion-controlled process as observed.[8] In contrast, photoexcitation at 390 nm

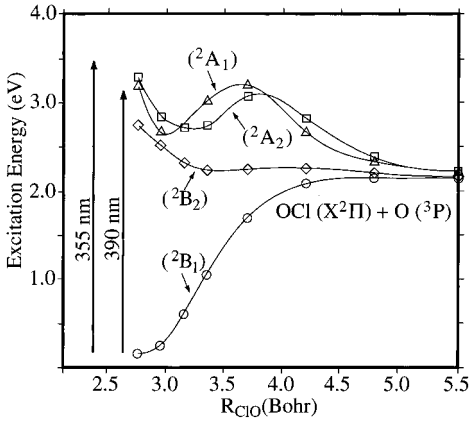

Figure 6. Potential energy curves for the first four electronic states of ClO_2 calculated by Peterson and Werner[16] at varying lengths of one ClO bond, while the other has the equilibrium length characteristic of the ground state. Arrows indicate the excitation energies at 355 and 390 nm.

may generate $ClO_2(^2A_2)$ with insufficient energy to cross the barrier, and in that case the system will convert to the unbound $^2B_2$ state, transferring some of the excess energy to the solvent in the process. As a result, little or no excess energy is retained to separate the fragments ClO and O, and a fast geminate recombination, producing ClO_2 in the electronic ground state, becomes the dominant mode of relaxation. No corresponding wavelength dependence of the cage escape is expected for Cl + O_2, since these products descend from the $^2B_2$ state with an excess energy of several electronvolts.

This argument, based on the gas-phase energetics, should be valid also in aqueous solution because the hydration energies of the neutral species involved are very moderate. Thus, the contribution from hydration to the energy change of the process $ClO_2(^2B_2) \rightarrow ClO + O$ has been estimated to be (+)0.1 eV.[6]

Interpretation of the Time Evolution of the Transient Absorptions. The discussion above leads to the conclusion that two relaxation channels are available for the $^2B_2$ state of ClO_2 in aqueous solution:

$$ClO_2(^2B_2) \rightarrow ClO_2(^2B_1) \quad (90\%) \tag{7}$$

and

$$ClO_2(^2B_2) \rightarrow Cl + O_2 \quad (10\%) \tag{8}$$

Assuming that the $^2B_2$ state becomes populated within the duration of the pump pulse and that the absorption of this state is negligible at the three wavelengths considered here, we ascribe the observed transient absorptions $\Delta A(t)$ to the time evolution of the absorption of $ClO_2(^2B_2)$ undergoing relaxation processes 7 and 8. The assignment of the various transient absorption signals to the two processes is made as follows. The transient at 780 nm clearly extends the series of transients observed in the range 400−700 nm by Chang and Simon[15] and successfully described by these authors as arising from the spectral shifts associated with the gradual relaxation of a vibrationally excited species. Chang and Simon argued that the relaxing species was ClOO. However, this assignment is inconsistent with our data at 260 nm, which show no sign of the rise in the absorbance after 5−10 ps that would necessarily accompany the completion of the vibrational relaxation of ClOO. Noting that $ClO_2(^2B_1)$ should be formed in process 7 with an excess (vibrational) energy of about 2 eV (see Figure 6), we therefore assign the transient at 780 nm to the vibrational relaxation of $ClO_2(^2B_1)$. To be consistent with the rise time of the transient, this assignment implies that the formation of $ClO_2(^2B_1)$ is completed within about 1 ps. Hence, we are led to ascribe the 10 ps recovery of the absorbance at 390 nm to the relaxation of $ClO_2(^2B_1)$ via successive vibrational levels rather than to the formation of this species itself. The fast-decaying component of the transient at 260 nm has a time constant that is consistent with the upper limit for the time of formation of $ClO_2(^2B_1)$ set by the rise time of the 780 nm transient. We therefore assign this component to the initial stage of process 7 preceding the vibrational relaxation of $ClO_2(^2B_1)$, while the slowly decaying component at 260 nm is assigned to process 8.

The three observed $\Delta A(t)$ can be expressed with fair accuracy in terms of a few exponentials each. Accordingly, they may be formally described as representing the formation and decay in first-order processes of intermediate species having time-independent extinction coefficients. This interpretation allows a concise description and a simulation of the transients in terms of a mechanism consisting of a set of rate constants and extinction coefficients of intermediates and products. However, owing to the very short lifetimes of the postulated intermediates, their actual existence as well-defined chemical species is not implied. Adopting this picture, we assign the transient at 780 nm to the formation and decay of a single, excited vibrational state of $ClO_2(^2B_1)$, and the recovery of the absorbance at 390 nm to the formation of $ClO_2(^2B_1)$ in the vibrational ground state, superimposed on the formation of Cl atoms. We thus make the somewhat unrealistic assumption that none of the vibrationally excited states of $ClO_2(^2B_1)$ absorb at 390 nm, although the recovery of the absorbance probably involves contributions from the successive population and depopulation of a substantial number of vibrational states. The fast-decaying component at 260 nm is assigned to the formation and decay of a precursor for $ClO_2(^2B_1)$, which we label ClO + O in accordance with the discussion in the preceding section, while the slowly decaying component is taken to represent the formation of Cl atoms via an unidentified precursor P. According to this assignment, the decay time of the component associated with the intermediate ClO + O becomes the time of geminate recombination of ClO and O. We note, however, that the subpicosecond lifetime of ClO + O suggests that ClO and O never really separate. Rather, process 7 may be visualized as an asymmetric distortion of $ClO_2(^2B_2)$ that approaches the ClO + O asymptote, where crossing to the $ClO_2(^2B_1)$ surface is facilitated by the near-degeneracy of the two states (Figure 6). Similarly, the formation and decay of the precursor P may in fact represent a sequence of nonequilibrium configurations connecting $ClO_2(^2B_2)$ with the products Cl + O_2.

In accordance with the assignments made above, we represent the transient absorptions $\Delta A(t)$ in terms of the mechanism

$$ClO_2(^2B_2) \xrightarrow{k_P} P \xrightarrow{k_{Cl}} Cl + O_2$$

$$ClO_2(^2B_2) \xrightarrow{k_{ClO}} ClO + O \xrightarrow{k_3} ClO_2^{(3)} \xrightarrow{k_2} ClO_2^{(2)} \xrightarrow{k_1} ClO_2^{(1)} \xrightarrow{k_0} ClO_2^{(0)} \tag{9}$$

where $ClO_2^{(i)}$, $i = 1, 2, 3$, denote typical vibrational states of $ClO_2(^2B_1)$ of increasing vibrational energy and $ClO_2^{(0)}$ is the vibrational ground state. The transients at 780, 390, and 260 nm are ascribed to $ClO_2^{(2)}$, to $ClO_2^{(0)}$ and Cl, and to ClO + O, P, and Cl, respectively.

The rate constants and the extinction coefficients at 260 nm of the short-lived intermediates ClO + O and P, as well as that of $ClO_2^{(2)}$ at 780 nm, were determined by fitting a simulation to the observed $\Delta A(t)$. The extinction coefficients of Cl and $ClO_2^{(0)}$ were those listed in Table 1. The initial concentration of $ClO_2(^2B_2)$, equal to the deficit of $ClO_2(^2B_1)$, was derived from the initial bleaching at 390 nm, and the ratio of the constants k_P and k_{ClO} was fixed by requiring $\Phi(Cl) = 0.1$. The contribution to $\Delta A(t)$ from the two-beam coupling at $t = 0$ was in each case simulated by adding a Gaussian centered at $t = 0$ and having the width of the laser pulse. Moreover, the fast-decaying anisotropy depicted in Figure 5 was included in the simulation of the transient at 390 nm. Finally, the calculated functions $\Delta A(t)$ were convolved with the Gaussian shape of the probe pulse. The resulting curves are shown in Figures 2−4, superimposed on their experimental counterparts. A very satisfactory fit to the measured time evolution of all three transients is obtained, confirming the consistency of assumed mechanism 9 with the available data. In particular, the simulation indicates that the rate of formation of Cl corresponds to the rate of decay of P, thus supporting the assumed relationship between P and Cl. As a further test, we have calculated the transient at 350 nm with the same set of rate constants for comparison with the transient data recorded at this

TABLE 2: Rate Constants (in ps^{-1}) and Extinction Coefficients of Intermediate Species Used with Eq 9 to Simulate the Transient Absorptions

k_P	k_{ClO}	k_{Cl}	k_3	k_2	k_1	k_0
0.28	2.5	0.24	2.1	1.5	1.0	0.125

	ϵ [L cm^{-1} mol^{-1}]			
	260 nm	350 nm	390 nm	780 nm
$ClO_2^{(2)}$	0	0	0	170
ClO + O	800	0	0	0
P	7200	0	0	0

wavelength by Chang and Simon (see Figure 1 of ref 15). We note that the simulated curve, shown in Figure 3, correctly crosses the abscissa near 20 ps delay and exhibits the expected ratio of $\Delta A(t = 0)$ and $\Delta A(t = 60$ ps).

The rate constants and extinction coefficients obtained from the simulation are listed in Table 2. The value of the extinction coefficient of the intermediate labeled ClO + O is close to the equilibrium value of ϵ_{ClO} at 260 nm (Table 1), thus justifying the assignment. Moreover, the value of k_3, representing the rate of decay of ClO + O, is consistent with the rate expected for geminate recombination dominated by single collision of the photofragments with the solvent cage.[24] The precursor P for the Cl atom absorbs strongly at 260 nm, the extinction coefficient being of the order of magnitude as that of ClOO (Table 1). Hence, it is tempting to propose that $ClO_2(^2B_2)$ approaches a configuration resembling ClOO before dissociating into Cl + O_2 at a rate given by k_{Cl}. However, since the lifetime $(k_{Cl})^{-1}$ of P is only 3% of the reported lifetime of ClOO in aqueous solution,[8] additional observations are required to determine the nature of this intermediate.

Interpretation of the Polarization Data at 390 nm. The observation of a photoinduced dichroism at 390 nm where $ClO_2(^2B_1)$ absorbs strongly, but not at 260 and 780 nm where the absorptions of the photoproducts dominate, immediately suggests that the dichroism arises from the expected preferential depletion of those ClO_2 molecules oriented with the transition dipole moment (i.e., the O−O direction) parallel to the electric vector of the pump beam. Hence, we assign the dichroism to an orientational anisotropy of the ClO_2 molecules remaining in the electronic ground state after the termination of the pump pulse.

It appears from Figure 5 that the initial value of the anisotropy $r(t)$ exceeds somewhat the value $r(0) = 2/5$ characteristic of the orientational anisotropy created by preferential depletion. However, since the strong initial transients due to two-beam coupling are very different for parallel and perpendicular polarizations of the beams, the determination of $r(t)$ within the first 0.3 ps is inaccurate. The calculated curve shown in Figure 5 represents an exponential decay with a time constant of 0.6 ps, delayed 0.3 ps with respect to $t = 0$ and convolved with a Gaussian pulse shape of width 150 fs. The fit to the observed $r(t)$ is approximate only, implying a substantial uncertainty (±0.2 ps) in the determination of the time constant. However, the accuracy of the data hardly warrants the introduction of additional parameters to improve the fit.

The very fast decay of $r(t)$ indicates that ClO_2 moves almost independently of the surrounding water molecules. This suggests that the rotational motion of ClO_2 may be described either in terms of a free rotor or by the hydrodynamic slip model.[25] An effective orientational relaxation time for free rotation can be defined as[25]

$$\tau_{free} = \frac{2\pi}{9}\sqrt{\frac{I}{kT}} \qquad (10)$$

TABLE 3: Comparison of the Photolysis of Aqueous ClO_2 and O_3^- at 390 nm

	ClO_2[a]	O_3^-[b]
main photolytic process	OClO → ClO + O	$O_3^- \rightarrow O^- + O_2$
ΔE_e (eV)[c]	0 [i]	2.5
Φ_{ce}[d]	0	0.5
$(k_r)^{-1}$ (ps)[e]	0.5	3.5
E_v (eV)[f]	2.0	0.3
τ_v (ps)[g]	8	≪3.5
τ_R (ps)[h]	0.5	2.3

[a] This work. [b] Data from ref 17. [c] Excess electronic energy. [d] Quantum yield for cage escape. [e] Time constant for geminate recombination. [f] Maximum vibrational energy after recombination. [g] Time constant for vibrational relaxation. [h] Time constant for rotational relaxation. [i] Assuming that the dissociation proceeds from the $^2B_2$ state. Energies of hydration neglected.

where I is the moment of inertia, k is the Boltzmann constant, and T is the temperature. ClO_2 is an almost symmetric top with rotational constants $A = 1.74$ cm^{-1}, $B = 0.33$ cm^{-1}, and $C = 0.28$ cm^{-1}. Since the electronic transition is polarized along the A-axis, rotation about both the B- and the C-axis will change the anisotropy. Ignoring the small inequivalence of B and C, we obtain from eq 10 the value $\tau_{free} = 0.36$ ps, which is about half the measured reorientation time.

In the hydrodynamic slip model the rotational motion is governed by a friction between the solvent and the solute, taken to arise from the displacement of solvent molecules by the rotation of the nonspherical solute. Therefore, the rotational relaxation does not depend on the moments of inertia but on the volume and shape of the solute, which is represented as a smooth ellipsoid. The volume of ClO_2, determined from the geometry[26] $r_{ClO} = 1.475$ Å and $\theta = 117.6°$ and the van der Waals radii of chlorine and oxygen (1.8 and 1.4 Å, respectively), is $V = 33.5$ Å^3, and the "length" of the molecule is 5.32 Å. We represent ClO_2 as a prolate spheroid with the long axis equal to the calculated length of the molecule and with the short axis chosen to reproduce the calculated volume. The transition dipole moment is parallel to the long axis. For this simplified case the decay of the anisotropy caused by the hydrodynamic slip reorientation is expressed:[27]

$$r(t) = \frac{2}{5}\exp\left(-\frac{6kT}{\eta V \lambda_\perp}t\right) \qquad (11)$$

where η is the viscosity of the solvent ($\eta = 0.890 \times 10^{-3}$ kg/ms for water at 298 K)[28] and $\lambda_\perp$ is the friction coefficient, which has been tabulated as a function of the axial ratio of the spheroid.[29] With the axial ratio $R = 0.65$ we obtain $\lambda_\perp = 0.445$ and, hence, $r(t) = 2/5\ \exp(-t/0.54$ ps), in agreement with the measured decay. We thus conclude that the slip model accounts for the observed orientational relaxation of ClO_2 in water.

Comparison with the Photolysis of O_3^- in Aqueous Solution. A femtosecond study of the photolysis at 390 nm of O_3^- in aqueous solution was reported recently by Barbara and co-workers.[17] O_3^- and ClO_2 are isoelectronic radicals with similar geometries as well as similar electronic and vibrational spectra. Moreover, the main process of the near-ultraviolet photolysis in the gas phase is for both species a dissociation, splitting off an outer atom. Accordingly, any differences between the photodynamics of ClO_2 and O_3^- observed in aqeuous solution may be expected to arise from the stronger interaction of charged solutes with the polar solvent compared to that of neutral solutes. In Table 3 the results obtained for ClO_2 and O_3^- are compiled. The large difference beween the observed quantum yields for cage escape and between the rates of geminate recombination may both be ascribed to the very

different amount of excess energy $\Delta E_e$of the photoproducts: while ClO + O arise from the unbound $^2B_2$ state of ClO_2 with no kinetic energy and, therefore, recombine completely in a very fast process of the single-collision type, $O^- + O_2$, arising from the strongly dissociative $^2A_2$ state of O_3^-,[17] acquire sufficient kinetic energy to penetrate the cage. Hence, $O_2 + O^-$ either escape permanently or recombine in a comparatively slow, diffusion-like process.[24]

Since the electronic ground states of ClO_2 and O_3^- both have vibrational bands near 1000 cm^{-1}, which are expected to couple to a librational band of water,[30] both species should exhibit an efficient vibrational relaxation. The finding that the relaxation of O_3^- is at least an order of magnitude faster than that of ClO_2 therefore suggests an enhancement attributable to the much stronger Coulomb interaction of the charged species with the polar solvent. We note, however, that the initial vibrational energy of the regenerated molecule is significantly lower for O_3^- than for ClO_2, which may increase the apparent difference between the relaxation rates.

The rates of rotational relaxation similarly reflect the difference in the solute−solvent interaction. The observed rate for ClO_2 is in accord with the slip model, whereas the slower reorientation of O_3^- indicates a stronger interaction with the solvent.

Conclusions

The main result of the present investigation of the photolysis of aqueous ClO_2 at 390 nm is that, in contrast to previously reported results, chlorine atoms formed with a quantum yield of 0.1 are the only product detectable 25 ps after the photolysis pulse. The major product of the preliminary photolysis, ClO + O, disappears through fast geminate recombination to vibrationally excited ClO_2 in the electronic ground state. Hence, the ClO + O product channel from the unbound $^2B_2$ state, which accounts for more than 90% of the photolysis in the gas phase, is blocked in aquoues solution, since no excess energy is available to ensure the cage escape of the products.

The analysis of the time evolution of the transient observed at 260 nm suggests the presence of a short-lived precursor for the chlorine atom. Like ClOO, this precursor absorbs strongly at 260 nm. However, since the lifetime (4 ps) is inconsistent with that reported for ClOO, the precursor remains unidentified. Since no evidence for the expected formation of ClOO was obtained in the present experiments, the question of the direct photoisomerization of ClO_2 is still unsettled, and further work is required to determine the mechanism of the photolytic formation of Cl atoms from aqueous ClO_2 .

Acknowledgment. The authors thank U. Kläning for stimulating discussions and the Carlsberg Foundation and the SNF-Center for Molecular Reaction Dynamics and Laser Chemistry for financial support.

References and Notes

(1) Vaida, V; Solomon, S.; Richard, E. C.; Ruhl, E.; Jefferson, A. *Nature* **1989**, *342*, 405.
(2) Rühl, A.; Jefferson, A.; Vaida, V. *J. Phys. Chem*. **1990**, *94*, 2990.
(3) Davis, H. F.; Lee, Y. T. *J. Phys. Chem.* **1992**, *96*, 5681.
(4) Bishenden, E.; Donaldson, D. J. J. *Chem. Phys*. **1993**, *99*, 3129.
(5) Baumert, T.; Herek, J. L.; Zewail, A. H. *J. Chem. Phys*. **1993**, *99*, 4430.
(6) Vaida, V.; Simon, J. D. *Science* **1995**, *268*, 1443.
(7) Dunn, R. C.; Richard, E. C.; Vaida, V.; Simon, J. D. *J. Phys. Chem*. **1991**, *95***,** 6060
(8) Dunn, R. C.; Simon, J. D. *J. Am. Chem. Soc.* **1992**, *114*, 4856.
(9) Dunn, R. C.; Flanders, B. N.; Simon, J. D. *J. Phys. Chem.* **1995**, *99*, 7360.
(10) Dunn, R. C.; Anderson, J.; Foote, C. S.; Simon, J. D. *J. Am. Chem. Soc.* **1993**, *115*, 5307.
(11) Jafri, J. A.; Lengsfield, B. H., III; Bauschlicher, C. W., Jr.; Phillips, D. H. *J. Chem. Phys*. **1985**, *83*, 1693.
(12) Johnston, H. S.; Morris, E. D.; Van den Bogaerde, J. *J. Am. Chem. Soc.* **1969**, *91*, 7712.
(13) Mauldin, R. L., III; Burkholder, J. B.; Ravishankara, A. R. *J. Phys. Chem.* **1992**, *96*, 2582.
(14) Müller, H. S. P.; Willner, H. *J. Phys. Chem*. **1993**, *97*, 10589.
(15) Chang, Y. J.; Simon, J. D. *J. Phys. Chem.* **1996**, *100*, 6406.
(16) Peterson, K. A.; Werner, H.-J. *J. Chem. Phys.* **1992**, *96*, 8948.
(17) Walhout, P. K.; Silva, C.; Barbara, P. F. *J. Phys. Chem.* **1996**, *100*, 5188.
(18) Bray, W. Z. *Phys. Chem*. **1906**, *54*, 569.
(19) Emerich, D. E. *Reactions of Oxychlorine Species in Aqueous Solution*; Miami University: Oxford, OH, 1981.
(20) Shank, C. V.; Ippen, E. P. *Appl. Phys. Lett*. **1975**, *26*, 62.
(21) Stitt, F.; Friedlander, S.; Lewis, H. J.; Young, F. E. *Anal. Chem*. **1954**, *26*, 1478.
(22) Buxton, G. V.; Subhami, M. S. *J. Chem. Soc., Faraday Trans 1* **1972**, *68*, 947.
(23) Kläning, U. K.; Wolf, T. *Ber. Bunsen-Ges. Phys. Chem.* **1985**, *89*, 243.
(24) Schwartz, B. J.; King, J. C.; Zhang, J. Z.; Harris, C. B. *Chem. Phys. Lett*. **1993**, *203*, 503.
(25) Myers, A. B.; Pereia, M. A.; Holt, P. L.; Hochstrasser, R. M. *J. Chem. Phys*. **86,** *95*.
(26) Clark, A. H. *J. Mol. Struct*. **1971**, *7*, 485.
(27) Fleming, G. R. *Chemical Applications of Ultrafast Spectroscopy*; Oxford University Press: New York, 1986; Chapter 6, p 124.
(28) *CRC Handbook of Physics and Chemistry* 73rd ed.; CRC Press: Boca Raton, FL, 1993; pp 6−166.
(29) Youngren, G. K.; Acrivos, A. J. *Chem. Phys*. **1975,** *63*, 3846.
(30) Whitnell, R. M.; Wilson, K. R.; Hynes, J. T. *J. Chem. Phys.* **1992**, *96*, 5354.